

Observation of New Charmless Decays of Bottom Hadrons

MICHAEL J. MORELLO⁽¹⁾(*)

⁽¹⁾ *Fermi National Accelerator Laboratory*

Summary. — We search for new charmless decays of neutral b -hadrons to pairs of charged hadrons with the upgraded Collider Detector at the Fermilab Tevatron. Using a data sample corresponding to 1fb^{-1} of integrated luminosity, we report the first observation of the $B_s^0 \rightarrow K^- \pi^+$ decay, with a significance of 8.2σ , and measure $\mathcal{B}(B_s^0 \rightarrow K^- \pi^+) = (5.0 \pm 0.7 \text{ (stat.)} \pm 0.8 \text{ (syst.)}) \times 10^{-6}$. We also report the first observation of charmless b -baryon decays in the channels $\Lambda_b^0 \rightarrow p\pi^-$ and $\Lambda_b^0 \rightarrow pK^-$ with significances of 6.0σ and 11.5σ respectively, and we measure $\mathcal{B}(\Lambda_b^0 \rightarrow p\pi^-) = (3.5 \pm 0.6 \text{ (stat.)} \pm 0.9 \text{ (syst.)}) \times 10^{-6}$ and $\mathcal{B}(\Lambda_b^0 \rightarrow pK^-) = (5.6 \pm 0.8 \text{ (stat.)} \pm 1.5 \text{ (syst.)}) \times 10^{-6}$. No evidence is found for the decays $B^0 \rightarrow K^+ K^-$ and $B_s^0 \rightarrow \pi^+ \pi^-$, and we set an improved upper limit $\mathcal{B}(B_s^0 \rightarrow \pi^+ \pi^-) < 1.2 \times 10^{-6}$ at the 90% confidence level. All quoted branching fractions are measured using $\mathcal{B}(B^0 \rightarrow K^+ \pi^-)$ as a reference.

PACS 13.25.Hw – Decays of bottom mesons.

PACS 13.30.Eg – Hadronic decays.

1. – Introduction

Non-leptonic two-body charmless decays of neutral b hadrons ($B^0 \rightarrow h^+ h'^-$, $B_s^0 \rightarrow h^+ h'^-$ and $\Lambda_b^0 \rightarrow ph^-$, where h is a charged pion or kaon) are very interesting for the understanding of flavor physics and CP violation mechanism in the b -hadron sector. Their rich phenomenology offers several opportunities to explore and constrain the parameters of the quark-mixing matrix (i.e. Cabibbo-Kobayashi-Maskawa, CKM). These processes allow to access the phase of the V_{ub} element of the CKM matrix (γ angle), and to test the reliability of the Standard Model (SM) and hadronic calculations. The presence of New Physics can be revealed by its impact on their decay amplitudes, where new particles may enter in penguin diagrams. The $B^0 \rightarrow K^+ \pi^-$ is the first process involving the b quark where direct CP violation has been observed.

The measurements obtained at e^+e^- colliders (ARGUS, CLEO, LEP, and more recently, BaBar and Belle experiments) already provided a wealth of results for B^0 and B^+

(*) morello@fnal.gov

mesons. The upgraded Collider Detector at the Fermilab Tevatron (CDF II), with its large production of b -hadrons is in principle an ideal environment for studying these rare modes. In addition to providing further large samples of B^0 and B^+ mesons in a different experimental environment, it provides the exciting opportunity of studying the charmless decays of other b -hadrons that are unaccessible (or much less accessible) in other experiments. A variety of techniques have been proposed to constrain the CKM parameters or probe effects of New Physics [1, 2, 3, 4] exploiting a combination of observables from B_s^0 and B^0 , B^+ mesons.

The $B_s^0 \rightarrow K^-\pi^+$ decay offers several and interesting strategies to extract useful information from the comparison between its observables and those of its U-spin related partner $B^0 \rightarrow K^+\pi^-$ [3, 4]. By combining the information of rates and direct CP asymmetries of U-spin-related decays $B^0 \rightarrow K^+\pi^-$ and $B_s^0 \rightarrow K^-\pi^+$ [3, 4] allows a stringent test of the Standard Model origin of the $\mathcal{O}(10\%)$ direct CP asymmetry observed in $B^0 \rightarrow K^+\pi^-$ [8], which is not matched by a similar effect in the $B^+ \rightarrow K^+\pi^0$ decay, which differs only by the spectator quark. This raised discussions about a possible exotic source for the CP violation in the $B^0 \rightarrow K^+\pi^-$ decay [9, 10, 11]. Any significant disagreement between the measured partial rate asymmetries of strange and non-strange b -meson $K\pi$ decays should be strong indication of New Physics.

The $B_s^0 \rightarrow K^-\pi^+$ is still unobserved and the current experimental upper limit $\mathcal{B}(B_s^0 \rightarrow K^-\pi^+) < 5.6 \times 10^{-6}$ @ 90% CL [5] from CDF is very close to (sometimes lower than) the current theoretical expectations [12, 13, 14, 15]. The comparison of this branching fraction, sensitive to CKM angle values of α and γ [14], with theoretical predictions provides valuable information for tuning the phenomenological models of hadronic $B_{(s)}^0$ decays and for optimizing the choice of their input parameters. Therefore, in this context the measurement of the decay rate of the $B_s^0 \rightarrow K^-\pi^+$ and the measurement of its direct CP asymmetry becomes crucial.

The amplitudes of penguin-annihilation and exchange diagrams, in which all initial-state quarks undergo a transition, are difficult to predict with current phenomenological models. In general they may carry different CP-violating and CP-conserving phases with respect to the leading processes, thereby influencing the determination of CKM-related parameters. The $B^0 \rightarrow K^+K^-$ and $B_s^0 \rightarrow \pi^+\pi^-$ decays proceed only through these kinds of diagrams. A simultaneous measurement of their decay rates (or improved constraints on them) would provide valuable estimates of the magnitude of these contributions [16].

Simultaneous measurements of $B_{(s)}^0 \rightarrow h^+h'^-$ observables, in most cases, exploit the U-spin symmetries to partially cancel out or constrain hadronic uncertainties and probe the electroweak and QCD structure. U-spin symmetry is not exactly conserved in the Standard Model and the magnitude of its violation is not precisely known but most authors estimate a $\mathcal{O}(10\%)$ effect. The $B_{(s)}^0 \rightarrow h^+h'^-$ system is a privileged laboratory since it offers the simultaneous opportunities of using U-spin assumptions and, at the same time, of checking their validity by measuring the symmetry breaking-size, from the interplaying of several U-spin-related observables.

Two-body charmless decays are also expected from bottom baryons. The modes $\Lambda_b^0 \rightarrow pK^-$ and $\Lambda_b^0 \rightarrow p\pi^-$ are predicted to have measurable branching fractions, of order 10^{-6} [17], and, in addition to the interest in their observation, must be considered as a possible background to the rare B_s^0 and B^0 modes being investigated.

In this Letter we report the results of a search for rare decays of neutral bottom hadrons into a pair of charged charmless hadrons (p , K or π), performed in 1fb^{-1} of $p\bar{p}$ collisions at $\sqrt{s} = 1.96$ TeV, collected by the upgraded Collider Detector (CDF II) at the

Fermilab Tevatron. We report the first observation of modes $B_s^0 \rightarrow K^- \pi^+$, $\Lambda_b^0 \rightarrow p K^-$, and $\Lambda_b^0 \rightarrow p \pi^-$, and measure their relative branching fractions. This is a short overview of the work documented in Ref. [18] and the results were published in [19].

Throughout this paper, C-conjugate modes are implied and branching fractions indicate CP-averages unless otherwise stated.

2. – CDF II detector

The CDF II detector [20, 21], in operation since 2001, is an azimuthally and forward-backward symmetric apparatus designed to study $p\bar{p}$ collisions at the Tevatron. It is a general purpose solenoidal detector which combines precision charged particle tracking with fast projective calorimetry and fine grained muon detection. Tracking systems are contained in a superconducting solenoid, 1.5 m in radius and 4.8 m in length, which generates a 1.4 T magnetic field parallel to the beam axis. Calorimetry and muon systems are all outside the solenoid. The main features of the detector systems are summarized below.

The tracking system consists of a silicon microstrip system [22] and of an open-cell wire drift chamber [23] that surrounds the silicon. The silicon microstrip detector consists of seven layers (eight layers for $1.0 < |\eta| < 2.0$) in a barrel geometry that extends from a radius of $r = 1.5$ cm from the beam line to $r = 28$ cm. The layer closest to the beam pipe is a radiation-hard, single sided detector called Layer $\emptyset\emptyset$ which employs sensors supporting high-bias voltages. This enables signal-to-noise performance even after extreme radiation doses. The remaining seven layers are radiation-hard, double sided detectors. The first five layers after Layer $\emptyset\emptyset$ comprise the Silicon Vertex II (SVXII) detector and the two outer layers comprise the Intermediate Silicon Layer (ISL) system. This entire system allows track reconstruction in three dimensions. The impact parameter resolution of the combination of SVXII and ISL is about $48 \mu\text{m}$ including a $30 \mu\text{m}$ contribution from the beamline for tracks with transverse momentum of $2 \text{ GeV}/c$. The z_0 resolution of the SVXII and ISL is $70 \mu\text{m}$. The 3.1 m long cylindrical drift chamber (COT) covers the radial range from 40 to 137 cm and provides 96 measurement layers, organized into alternating axial and $\pm 2^\circ$ stereo superlayers. The COT provides coverage for $|\eta| \leq 1$. The hit position resolution is approximately $140 \mu\text{m}$ and the momentum resolution $\sigma_{p_T}/p_T \simeq 0.15\% p_T/(\text{GeV}/c)$. This corresponds to an observed mass-widths of about $14 \text{ MeV}/c^2$ for the $J/\psi \rightarrow \mu^+ \mu^-$ decays, and of about $8 \text{ MeV}/c^2$ for the $D^0 \rightarrow K^- \pi^+$ decays. The specific energy loss by ionization (dE/dx) of charged particles in the COT can be measured from the amount of charge collected by each wire. This yields a nearly-constant separation of 1.5 standard deviations between pions and kaons over the range $2 < p_T < 10 \text{ GeV}/c$.

A Time-of-Flight (TOF) detector [24], based on plastic scintillators and fine-mesh photomultipliers is installed in a few centimeters clearance just outside the COT. The TOF resolution is ≈ 100 ps and it provides at least two standard deviation separation between K^\pm and π^\pm for momenta $p < 1.6 \text{ GeV}/c$.

Segmented electromagnetic and hadronic sampling calorimeters surround the tracking system and measure the energy flow of interacting particles in the pseudo-rapidity range $|\eta| < 3.64$. The central calorimeters (and the endwall hadronic calorimeter) cover the pseudorapidity range $|\eta| < 1.1(1.3)$. The central electromagnetic calorimeter [25] (CEM) uses lead sheets interspersed with polystyrene scintillator as the active medium and employs phototube readout. Its energy resolution is $13.5\%/\sqrt{E_T} \oplus 2\%$. The central hadronic calorimeter [26] (CHA) uses steel absorber interspersed with acrylic scintillator as the

active medium. Its energy resolution is $75\%/\sqrt{E_T} \oplus 3\%$. The plug calorimeters cover the pseudorapidity region $1.1 < |\eta| < 3.64$. They are sampling scintillator calorimeters which are read out with plastic fibers and phototubes. The energy resolution of the plug electromagnetic calorimeter [27] is $16\%/\sqrt{E} \oplus 1\%$. The energy resolution of the plug hadronic calorimeter is $74\%/\sqrt{E} \oplus 4\%$.

The muon system resides beyond the calorimetry. Four layers of planar drift chambers (CMU) detect muons with $p_T > 1.4$ GeV/c which penetrate the five absorption lengths of calorimeter steel. An additional four layers of planar drift chambers (CMP) instrument 0.6 m of steel outside the magnet return yoke and detect muons with $p_T > 2.0$ GeV/c. The CMU and CMP chambers each provide coverage in the pseudo-rapidity range $|\eta| < 0.6$. The Intermediate MUon detectors (IMU) are covering the region $1.0 < |\eta| < 1.5$.

The beam luminosity is determined by using gas Cherenkov counters located in the $3.7 < |\eta| < 4.7$ region which measure the average number of inelastic $p\bar{p}$ collisions per bunch crossing [28].

The trigger and data acquisition systems are designed to accommodate the high rates and large data volume of Run II. Based on preliminary information from tracking, calorimetry, and muon systems, the output of the first level of the trigger is used to limit the rate for accepted events to ≈ 18 kHz at the luminosity range of $3\text{-}7 \cdot 10^{31} \text{ cm}^{-2}\text{s}^{-1}$. At the next trigger stage, with more refined information and additional tracking information from the silicon detector, the rate is reduced further to ≈ 300 Hz. The third and final level of the trigger, with access to the complete event information, uses software algorithms and a computing farm, and reduces the output rate to ≈ 75 Hz, which is written to permanent storage.

The only physics objects used in this analysis are the tracks, then just tracking system has been used.

3. – Data sample

We analysed an integrated luminosity $\int \mathcal{L} dt \simeq 1 \text{ fb}^{-1}$ sample of pairs of oppositely-charged particles with $p_T > 2$ GeV/c and $p_{T1} + p_{T2} > 5.5$ GeV/c, used to form b -hadron candidates. The trigger required also a transverse opening angle $20^\circ < \Delta\phi < 135^\circ$ between the two tracks, to reject background from particle pairs within the same jet and from back-to-back jets. In addition, both charged particles were required to originate from a displaced vertex with a large impact parameter d ($100 \mu\text{m} < d < 1 \text{ mm}$), while the b -hadron candidate was required to be produced in the primary $p\bar{p}$ interaction ($d_B < 140 \mu\text{m}$) and to have travelled a transverse distance $L_T > 200 \mu\text{m}$.

The offline selection is based on a more accurate determination of the same quantities used in the trigger, with the addition of two further observables: the isolation (I_B) of the candidate [29], and the quality of the three-dimensional fit (χ^2 with 1 d.o.f.) of the decay vertex of candidate. Requiring a large value of I_B reduces the background from light-quark jets, and a low χ^2 reduces the background from decays of different long-lived particles within the event, owing to the good resolution of the SVX detector in the z direction.

In the offline analysis, an unbiased optimization procedure determined a tightened selection on track-pairs fit to a common decay vertex. We chose the selection cuts minimizing directly the expected uncertainty of the physics observables to be measured. The selection is optimized for detection of the $B_s^0 \rightarrow K^- \pi^+$ mode. Maximal sensitivity for both discovery and limit setting is achieved with a single choice of selection requirements [30] by minimizing the variance of the estimate of the branching fraction in the

absence of signal [18]. The variance is evaluated by performing the full measurement procedure on simulated samples containing background and all signals from the known modes, but no $B_s^0 \rightarrow K^- \pi^+$ signal. The variance has been parameterized with analytical functions of the signal yield (S) and background level (B), and the free parameters determined from analysis of pseudo-experiments reproducing the experimental circumstance of data. For each set of cuts, S was estimated from Monte Carlo simulation and normalized to the yield observed in data after the trigger selection, and B was extrapolated from the sidebands of the $\pi\pi$ -mass distribution in data. This procedure yields the final selection: $I_B > 0.525$, $\chi^2 < 5$, $d > 120 \mu\text{m}$, $d_B < 60 \mu\text{m}$, and $L_T > 350 \mu\text{m}$.

The resulting invariant- $\pi\pi$ -mass distribution (see Fig. 1) shows a clean signal of $B_{(s)}^0 \rightarrow h^+ h'^-$ decays. In spite of a good mass resolution ($\approx 22 \text{ MeV}/c^2$), the various signal decay modes overlap into an unresolved mass peak.

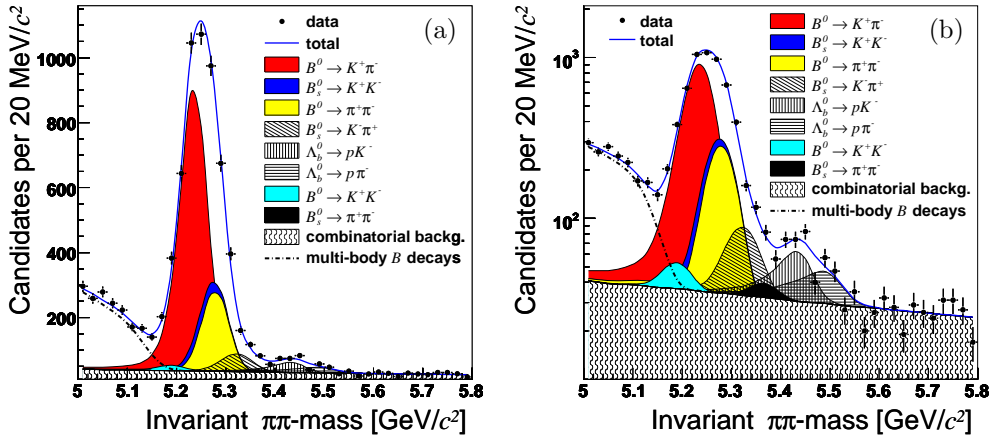


Fig. 1. – Invariant $\pi\pi$ -mass distribution of reconstructed candidates. The charged pion mass is assigned to both tracks. The total projection and projections of each signal and background component of the likelihood fit are overlaid on the data distribution. Signals and multi-body B background components are shown stacked on the combinatorial background component. Linear scale (a), logarithmic scale (b).

4. – Fit of composition

The resolution in invariant mass and in particle identification is not sufficient for separating the individual decay modes on an event-by-event basis, therefore we performed an unbinned maximum likelihood fit, combining kinematic and particle identification information to statistically determine both the contribution of each mode, and the relative contributions to the CP asymmetries. For the kinematic portion, we used three loosely correlated observables to summarize the information carried by all possible values of invariant mass of the b -hadron candidate, resulting from different mass assignments to the two outgoing particles [31]. They are: (a) the invariant $\pi\pi$ -mass $m_{\pi\pi}$ calculated with the charged pion mass assignment to both particles; (b) the signed momentum imbalance $\alpha = (1 - p_1/p_2)q_1$, where p_1 (p_2) is the lower (higher) of the particle momenta, and q_1 is the sign of the charge of the particle of momentum p_1 ; (c) the scalar sum of the particle

momenta $p_{tot} = p_1 + p_2$. Using these three variables, the mass of any particular mode $m_{m_1 m_2}$ ($m_{K\pi}, m_{\pi K}, m_{KK}, m_{p\pi}, m_{\pi p}, m_{pK}, m_{Kp}$) can be written as:

$$(1) \quad m_{m_1 m_2}^2 = m_{\pi\pi}^2 - 2m_\pi^2 + (m_1^2 + m_2^2) - 2\sqrt{p_1^2 + m_\pi^2} \cdot \sqrt{p_2^2 + m_\pi^2} + 2\sqrt{p_1^2 + m_1^2} \cdot \sqrt{p_2^2 + m_2^2},$$

$$(2) \quad p_1 = \frac{1 - |\alpha|}{2 - |\alpha|} p_{tot}, \quad p_2 = \frac{1}{2 - |\alpha|} p_{tot},$$

where m_1 (m_2) is the mass of the lower (higher) momentum particle. For simplicity, Eq. (1) is written as a function of p_1 and p_2 , but in the likelihood it was used as a function of α and p_{tot} . The simulated average values of $m_{\pi\pi}$ as a function of α for the twelve $B_s^0 \rightarrow h^+ h^-$ and $\Lambda_b^0 \rightarrow ph^-$ modes are shown in Fig. 2 and Fig. 3. Particle

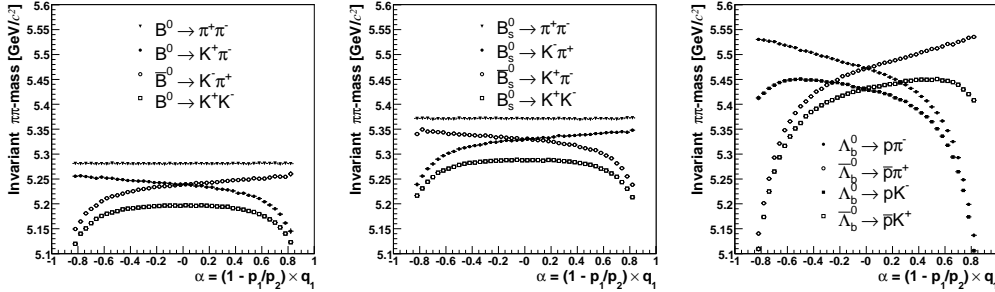


Fig. 2. – Average $m_{\pi\pi}$ versus α for simulated samples of B^0 , B_s^0 and Λ_b^0 decay modes.

identification (PID) information is summarized by a single observable kaonness $\kappa_{1(2)}$ for track 1(2), defined as

$$\kappa_{1(2)} = \frac{dE/dx_{1(2)} - dE/dx_{1(2)}(\pi)}{dE/dx_{1(2)}(K) - dE/dx_{1(2)}(\pi)},$$

where $dE/dx_{1(2)}(\pi)$ and $dE/dx_{1(2)}(K)$ are the expected $dE/dx_{1(2)}$ depositions for those particle assignments. With the chosen observables, the likelihood contribution of the i^{th} event is written as:

$$(3) \quad \mathcal{L}_i = (1 - f_b) \sum_j f_j \mathcal{L}_j^{\text{kin}} \mathcal{L}_j^{\text{PID}} + f_b (f_A \mathcal{L}_A^{\text{kin}} \mathcal{L}_A^{\text{PID}} + (1 - f_A) \mathcal{L}_C^{\text{kin}} \mathcal{L}_C^{\text{PID}})$$

where:

$$(4) \quad \mathcal{L}_j^{\text{kin}} = R_j(m_{\pi\pi} | \alpha, p_{tot}) P_j(\alpha, p_{tot}),$$

$$(5) \quad \mathcal{L}_A^{\text{kin}} = A(m_{\pi\pi}; c_2, m_0) P_A(\alpha, p_{tot}),$$

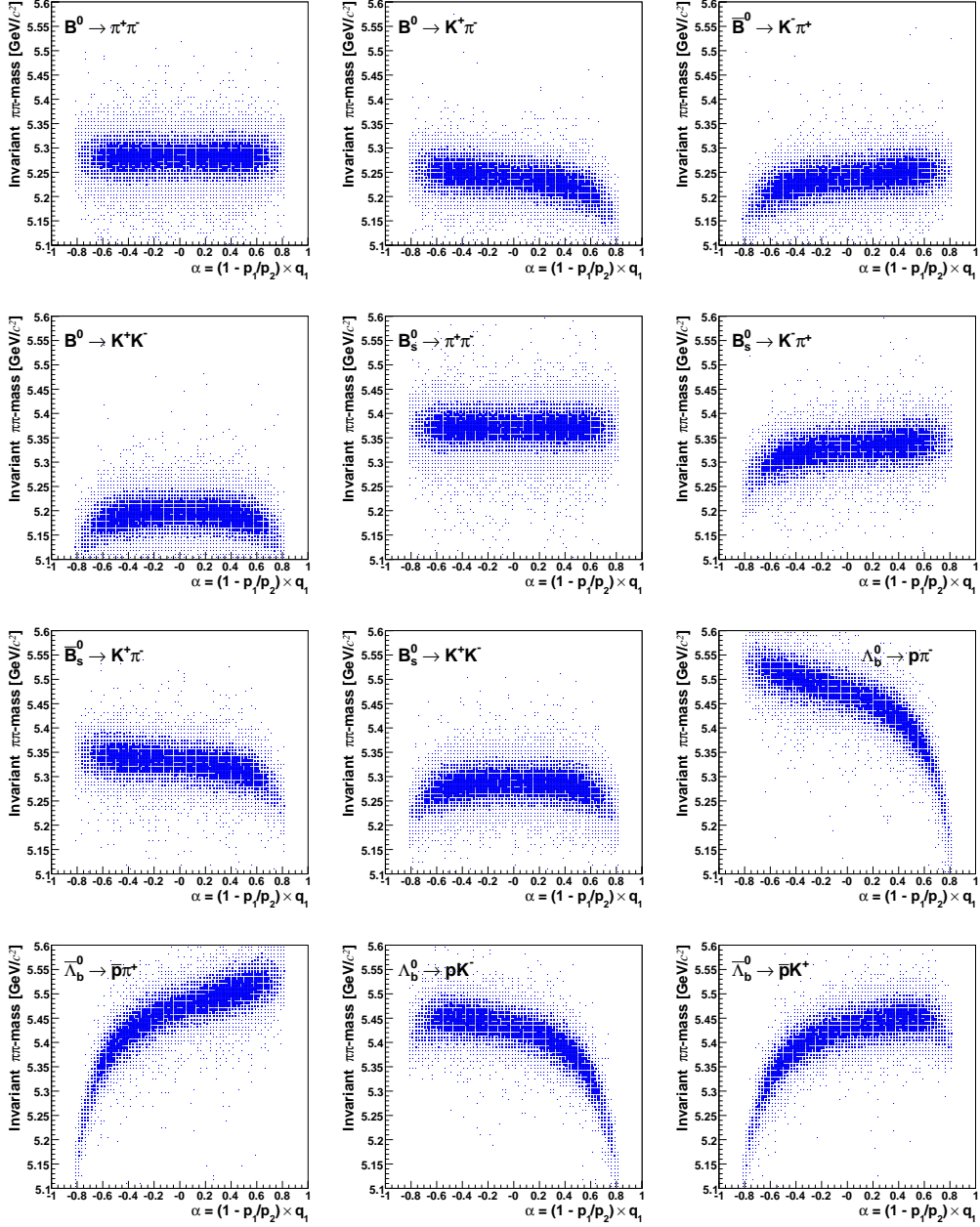


Fig. 3. $-m_{\pi\pi}$ versus α for simulated samples of $B_{(s)}^0 \rightarrow h^+ h'^-$ and $\Lambda_b^0 \rightarrow ph^-$ decay modes.

$$(6) \quad \mathcal{L}_C^{\text{kin}} = e^{c_1 m_{\pi\pi}} P_C(\alpha, p_{\text{tot}}),$$

$$(7) \quad \mathcal{L}_j^{\text{PID}} = F_j(\kappa_1, \kappa_2 | \alpha, p_{\text{tot}}),$$

$$(8) \quad \mathcal{L}_{A(C)}^{\text{PID}} = \sum_{l,m=e,\pi,K,p} w_l^{\text{A(C)}} w_m^{\text{A(C)}} F_{lm}(\kappa_1, \kappa_2 | \alpha, p_{\text{tot}}).$$

The various terms of the likelihood functions are described below.

The index j runs over the twelve distinguishable $B_{(s)}^0 \rightarrow h^+ h'^-$ and $\Lambda_b^0 \rightarrow ph^-$ modes, and f_j are their fractions to be determined by the fit, together with the total background fraction f_b . The background is composed of two different kinds: combinatorial background and partially-reconstructed heavy flavor decays. The combinatorial background is composed of random pairs of charged particle, displaced from the beam-line, accidentally satisfying the selection requirements, while the latter, referred as “physics” background, is composed of multi-body b -hadron decays (i.e. $B_{(s)}^0 \rightarrow \rho\pi/\rho K$) in which only two tracks are reconstructed. The indices A(C) label the physics (combinatorial) background quantities. The fraction of the physics background is given by f_A and it is a free parameter in the fit.

Each likelihood term, both for signals and backgrounds, is factorized into three different contributions: a) the conditional probability distribution of the invariant mass $m_{\pi\pi}$ given α and p_{tot} (for the background $m_{\pi\pi}$ is assumed to be independent of momentum), b) the joint conditional probability of PID variables κ_1, κ_2 given α, p_{tot} for a determined particles hypothesis, j in the case of signals (F_j) and l, m in the case of background ($F_{l,m}$), and c) the joint probability distribution of momentum variables α and p_{tot} ($P_{j(A,C)}$).

If $\mathcal{R}^j(m_j)$ is the mass resolution function of each mode j^{th} when the correct mass is assigned to both tracks, we can use Eq. (1) to change variable $m_j \rightarrow m_{\pi\pi}$ and to write the density probability function for each j^{th} decays mode as function of $m_{\pi\pi}$ given α and p_{tot} . In fact:

$$(9) \quad \mathcal{R}_j(m_j) = \mathcal{R}_j(m_j(m_{\pi\pi})) \cdot \frac{dm_{\pi\pi}}{dm_j} = R_j(m_{\pi\pi} | \alpha, p_{\text{tot}}).$$

The functional form of the mass resolution function $\mathcal{R}_j(m_j)$ was parameterized using the detailed detector simulation. To take into account non-Gaussian tails due to the emission of photons in the final state, we included soft photon emission in the simulation, using recent QED calculations [32]. The quality of the mass resolution model was verified by comparison data and simulation with about 1.5×10^6 tagged $D^0 \rightarrow K^- \pi^+$ decays reconstructed using the chain $D^{*+} \rightarrow D^0 \pi^+ \rightarrow [K^- \pi^+] \pi^+$ (see Fig. 4 and Fig. 5). The mass line-shape of the $D^0 \rightarrow K^- \pi^+$ was fitted by fixing the signal shape from the model, and allowing to vary only the background function. Good agreement was obtained between data and simulation. In Eq. (4), the nominal B^0, B_s^0 and Λ_b^0 masses measured by CDF [33] were used to reduce the systematic uncertainties related to the knowledge of the global mass scale.

The mass distribution of the physics background is parameterized with an “Argus function”, defined by the notation $A(m_{\pi\pi}; c_2, m_0)$ [34], convoluted with a Gaussian distribution centered at zero with a width, in this case, equal to the mass resolution, while the combinatorial background with an exponential function. The background mass distribution was determined in the fit by varying the parameters c_1, c_2 and m_0 in Eq. (5,6). The function $P_{j(A,C)}(\alpha, p_{\text{tot}})$ was parameterized by a product of polynomial and exponential functions fitted to Monte Carlo samples produced by a detailed detector simulation for each mode j , instead for the background terms was obtained from the mass sidebands of data [18].

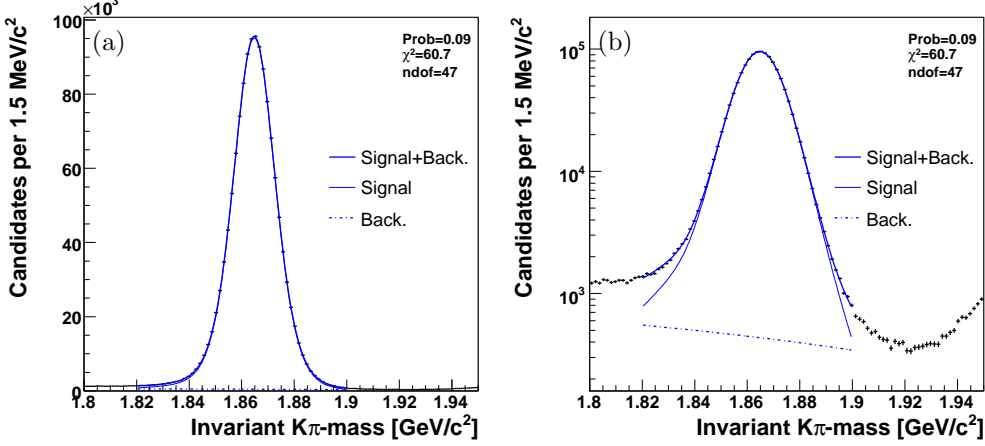


Fig. 4. – Invariant- $K\pi$ mass distribution for tagged $D^0 \rightarrow K^-\pi^+$ decays from $D^{*+} \rightarrow D^0\pi^+ \rightarrow [K^-\pi^+]\pi^+$. A verification of the mass line shape is superimposed, by performing a 1-D binned fit where the signal mass line shape is completely fixed from the model (see text). Linear scale (a), logarithmic scale (b).

The same data sample of 1.5×10^6 $D^{*+} \rightarrow D^0\pi^+ \rightarrow [K^-\pi^+]\pi^+$ decays used to test mass resolution model, where the D^0 decay products are identified by the charge of the D^{*+} pion, was used to calibrate the dE/dx response over the tracking volume and over time, and to determine the $F_{j(l,m)}(\kappa_1, \kappa_2|\alpha, p_{tot})$ functions in Eq. (7,8). In a $> 95\%$ pure D^0 sample, we obtained approximately 1.5σ separation between kaons and pions for particles with momentum larger than 2 GeV/c (see Fig. 6), corresponding to an uncertainty

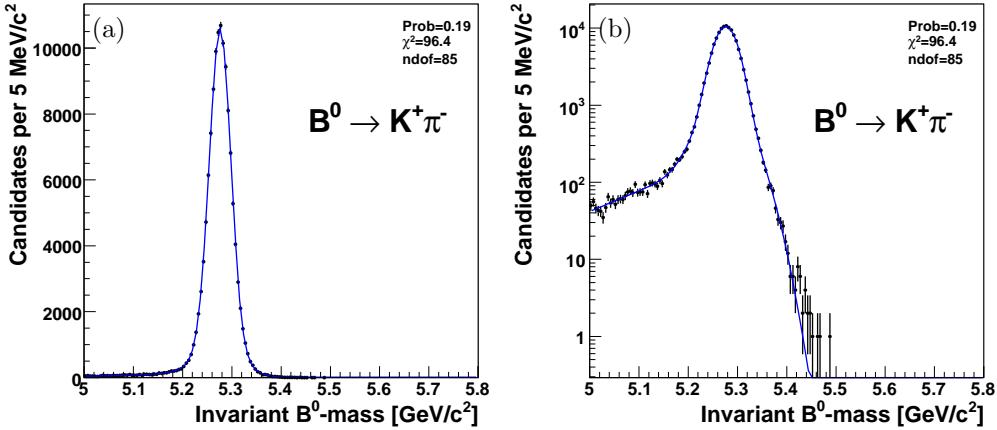


Fig. 5. – Invariant- $K\pi$ mass distribution of simulated $B^0 \rightarrow K^+\pi^-$ decays. The mass template is superimposed. Linear scale (a), logarithmic scale (b). Similar templates for all $B_{(s)}^0 \rightarrow h^+h'^-$ and $\Lambda_b^0 \rightarrow ph^-$ decay modes.

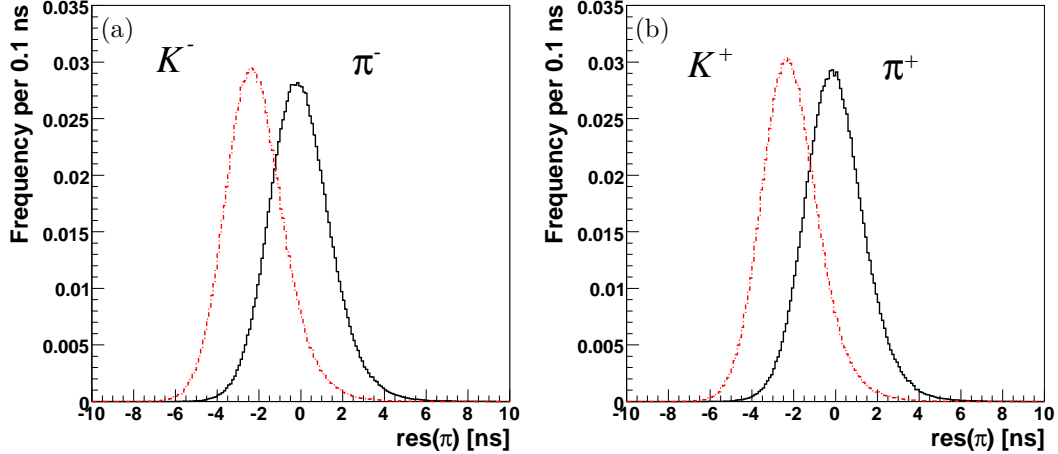


Fig. 6. – Distribution of dE/dx around the average pion response for negatively- (a) and positively- (b) charged particles. Pions (continuous line) and kaons (dashed line) from $D^0 \rightarrow K^- \pi^+$ decays.

on the measured fraction of each class of particles that is just 1.7 times worse than the uncertainty attainable with ideal separation between two classes of events completely disentangled. The effective separation among final states consisting in particle pairs, like in our case (between $\pi^+ \pi^-$ and $K^+ K^-$, between $\pi^+ K^-$ and $K^+ \pi^-$) corresponds to $1.5\sigma \cdot \sqrt{2} \simeq 2.1\sigma$, as shown in Fig. 7. This achievement is particularly crucial in separating those signal decay modes in which the kinematics does not sufficiently help.

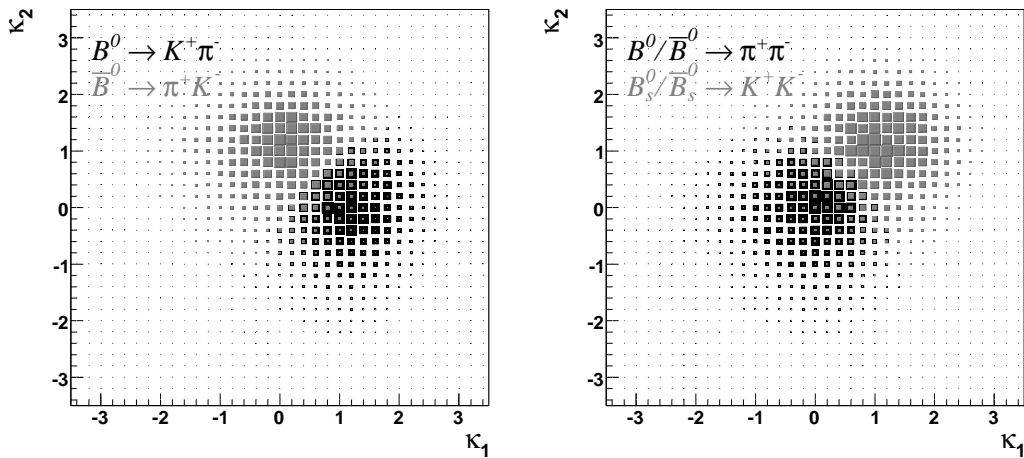


Fig. 7. – Probability density function $\int F_j(\kappa_1, \kappa_2 | \alpha, p_{tot}) P_j(\alpha, p_{tot}) d\alpha dp_{tot}$ for the some signal decays in the space $\alpha > 0$. To obtain the distributions for $\alpha < 0$ it is sufficient to invert $\kappa_1 \leftrightarrow \kappa_2$

TABLE I. – *Yields of signals returned from fits. For rare unobserved modes significance is quoted. The first quoted uncertainty is statistical, the second is systematic.*

Mode	N_s	Significance
$B_s^0 \rightarrow K^- \pi^+$	$230 \pm 34 \pm 16$	8.2σ
$B_s^0 \rightarrow \pi^+ \pi^-$	$26 \pm 16 \pm 14$	$< 3\sigma$
$B^0 \rightarrow K^+ K^-$	$61 \pm 25 \pm 35$	$< 3\sigma$
$\Lambda_b^0 \rightarrow p K^-$	$156 \pm 20 \pm 11$	11.5σ
$\Lambda_b^0 \rightarrow p \pi^-$	$110 \pm 18 \pm 16$	6.0σ

For example the kinematic separation power between the $B^0 \rightarrow \pi^+ \pi^-$ and $B_s^0 \rightarrow K^+ K^-$ modes is almost null, as shown in Fig. 2 and Fig. 3, while the dE/dx power separation is maximum, about 2.1σ , as shown in Fig. 7.

The dE/dx response of protons was determined from a sample of 124,000 $\Lambda \rightarrow p \pi^-$ decays, where the kinematics and the momentum threshold of the trigger allow unambiguous identification of the decay products [18].

The PID background term in Eq. (8) is similar to the signal terms, but allows for independent pion, kaon, proton, and electron components, which are free to vary independently for physics (combinatorial) background. In Eq. (8) the indices l and m run over the four possible particles e, π, K, p and the fractions of different kind of particles $w_l^{A(E)}, w_m^{A(E)}$ are free parameters in the fit. Muons are indistinguishable from pions with the available dE/dx resolution.

From the signal fractions returned by the likelihood fits we calculate the signal yields shown in Table I. The significance of rare unobserved signals is evaluated as the ratio of the yield observed in data, and its total uncertainty (statistical and systematic) as determined from a simulation where the size of that signal is set to zero. This evaluation assumes a Gaussian distribution of yield estimates, supported by the results obtained from repeated fits to simulated samples. This procedure yields a more accurate measure of significance with respect to the purely statistical estimate obtained from $\sqrt{-2\Delta\ln(\mathcal{L})}$. Significant signals are seen for $B^0 \rightarrow \pi^+ \pi^-$, $B^0 \rightarrow K^+ \pi^-$, and $B_s^0 \rightarrow K^+ K^-$, previously observed by CDF [5]. We obtain significant signals for the $B_s^0 \rightarrow K^- \pi^+$ mode (8.2σ), and for the $\Lambda_b^0 \rightarrow p \pi^-$ (6.0σ) and $\Lambda_b^0 \rightarrow p K^-$ (11.5σ) modes. Figure 8 shows relative likelihood distributions for these modes. No evidence is found for the modes $B_s^0 \rightarrow \pi^+ \pi^-$ or $B^0 \rightarrow K^+ K^-$, in agreement with expectations of significantly smaller branching fractions.

To avoid large uncertainties associated with production cross sections and absolute reconstruction efficiency, we measure all branching fractions relative to the $B^0 \rightarrow K^+ \pi^-$ mode. Frequentist upper limits [35] at the 90% C.L. are quoted for the unseen modes. For the measurement of Λ_b^0 branching fractions, the additional requirement $p_T(\Lambda_b^0) > 6$ GeV/ c was applied to allow easy comparison with other Λ_b^0 measurements at the Tevatron, which are only available above this threshold [36, 37]. This additional requirement lowers the Λ_b^0 yields by about 20%.

5. – Acceptance corrections and systematics

To convert the yields returned from the fit into relative branching fractions measurements, we applied corrections for efficiencies of trigger and offline selection requirements

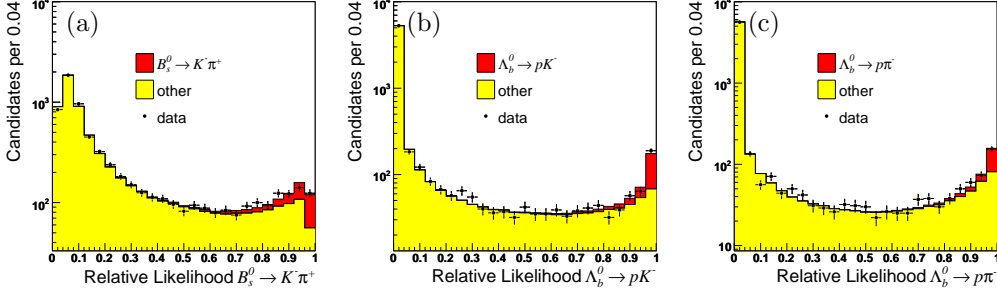


Fig. 8. – Distribution of the relative signal likelihood, $\mathcal{L}_S/(\mathcal{L}_S + \mathcal{L}_{\text{other}})$, in the region $5.1 < m_{\pi\pi} < 5.6 \text{ GeV}/c^2$. For each event, \mathcal{L}_S is the likelihood for the $B_s^0 \rightarrow K^- \pi^+$ (a), $\Lambda_b^0 \rightarrow p K^-$ (b), or $\Lambda_b^0 \rightarrow p \pi^-$ (c) signal hypotheses, and $\mathcal{L}_{\text{other}}$ is the likelihood for everything but the chosen signal, i.e. the weighted combination of all other components according to their measured fractions. Points with error bars show the distributions of data and histograms show the distributions predicted from the measured fractions.

for different decay modes. The relative efficiency corrections between modes do not exceed 8% for the measurements of b -mesons and 40% for Λ_b^0 branching fractions. Most corrections were determined from the detailed detector simulation, with some exceptions which were measured using data. A momentum-averaged relative isolation efficiency between B_s^0 and B^0 of 1.00 ± 0.03 was determined from fully-reconstructed samples of $B_s^0 \rightarrow J/\psi \phi$ and $B^0 \rightarrow J/\psi K^{*0}$ [18]. The lower specific ionization of kaons with respect to pions in the drift chamber is responsible for a $\simeq 5\%$ lower efficiency to reconstruct a kaon. This effect was measured in a sample of $D^+ \rightarrow K^- \pi^+ \pi^+$ decays triggered on two tracks, using the unbiased third track [38].

The $B_s^0 \rightarrow \pi^+ \pi^-$ modes required a special treatment, since it contains a superposition of the flavor eigenstates of the B_s^0 . Their time evolution might differ from the one of the flavor-specific modes if the width difference $\Delta\Gamma_s$ between the B_s^0 mass eigenstates is significant. The current result was derived under the assumption that both modes are dominated by the short-lived B_s^0 component, that $\Gamma_s = \Gamma_d$, and $\Delta\Gamma_s/\Gamma_s = 0.12 \pm 0.06$ [39, 40]. The latter uncertainty is included in estimating the overall systematic uncertainty.

The dominant contributions to the systematic uncertainty are the uncertainty on the combinatorial background model and the uncertainty on the dE/dx calibration and parameterization. Smaller systematic uncertainties are assigned for trigger efficiencies, physics background shape, kinematics, B meson masses and lifetimes.

6. – Results

The final results on branching fractions are listed in Table II, where f_d , f_s and f_Λ indicate the production fractions respectively of B^0 , B_s^0 and Λ_b^0 from fragmentation of a b quark in $p\bar{p}$ collisions. An upper limit is also quoted for modes in which no significant signal is observed [35]. We also list absolute results obtained by normalizing the data to the world-average of $\mathcal{B}(B^0 \rightarrow K^+ \pi^-)$ [43, 44]. The contributions from the likelihood fit for each decay mode are shown in Fig. 1.

The CP-averaged branching fraction of the newly observed mode $B_s^0 \rightarrow K^- \pi^+$ is

TABLE II. – Measured relative branching fractions of rare modes. The ratio f_Λ/f_d is p_T -dependent [37], and is defined here as: $f_\Lambda/f_d = \sigma(p\bar{p} \rightarrow \Lambda_b^0 X; p_T > 6 \text{ GeV}/c, |\eta| < 1)/\sigma(p\bar{p} \rightarrow B^0 X; p_T > 6 \text{ GeV}/c, |\eta| < 1)$. Absolute branching fractions were derived by normalizing to the current world-average value $\mathcal{B}(B^0 \rightarrow K^+\pi^-) = (19.4 \pm 0.6) \times 10^{-6}$, and assuming the average values at high energy for the production fractions: $f_s/f_d = 0.276 \pm 0.034$, and $f_\Lambda/f_d = 0.230 \pm 0.052$ [43]. The first quoted uncertainty is statistical, the second is systematic.

Mode		Relative \mathcal{B}	Absolute $\mathcal{B}(10^{-6})$
$B_s^0 \rightarrow K^-\pi^+$	$\frac{f_s}{f_d} \frac{\mathcal{B}(B^0 \rightarrow K^-\pi^+)}{\mathcal{B}(B^0 \rightarrow K^+\pi^-)}$	= $0.071 \pm 0.010 \pm 0.007$	$5.0 \pm 0.7 \pm 0.8$
$B_s^0 \rightarrow \pi^+\pi^-$	$\frac{f_s}{f_d} \frac{\mathcal{B}(B_s^0 \rightarrow \pi^+\pi^-)}{\mathcal{B}(B^0 \rightarrow K^+\pi^-)}$	= $0.007 \pm 0.004 \pm 0.005$	$0.49 \pm 0.28 \pm 0.36$ (< 1.2 at 90% C.L.)
$B^0 \rightarrow K^+K^-$	$\frac{\mathcal{B}(B^0 \rightarrow K^+K^-)}{\mathcal{B}(B^0 \rightarrow K^+\pi^-)}$	= $0.020 \pm 0.008 \pm 0.006$	$0.39 \pm 0.16 \pm 0.12$ (< 0.7 at 90% C.L.)
$\Lambda_b^0 \rightarrow pK^-$	$\frac{f_\Lambda}{f_d} \frac{\mathcal{B}(\Lambda_b^0 \rightarrow pK^-)}{\mathcal{B}(B^0 \rightarrow K^+\pi^-)}$	= $0.066 \pm 0.009 \pm 0.008$	$5.6 \pm 0.8 \pm 1.5$
$\Lambda_b^0 \rightarrow p\pi^-$	$\frac{f_\Lambda}{f_d} \frac{\mathcal{B}(\Lambda_b^0 \rightarrow p\pi^-)}{\mathcal{B}(B^0 \rightarrow K^+\pi^-)}$	= $0.042 \pm 0.007 \pm 0.006$	$3.5 \pm 0.6 \pm 0.9$

consistent with the previous upper limit ($< 5.6 \times 10^{-6}$ at 90% C.L.) based on a subsample of the current data [5], and agrees with the prediction in Ref. [15], but it is lower than most other predictions [12, 45, 46].

The $B_s^0 \rightarrow \pi^+\pi^-$ upper limit improves and supersedes the previous best limit [5]. The present measurement of $\mathcal{B}(B^0 \rightarrow K^+K^-)$ is in agreement with other existing measurements and has a similar resolution [43], but the resulting upper limit is weaker due to the observed central value. The sensitivity to both $B^0 \rightarrow K^+K^-$ and $B_s^0 \rightarrow \pi^+\pi^-$ is now close to the upper end of the theoretically expected range [12, 13, 14, 45, 47].

We also report the first branching fraction measurements of charmless Λ_b decays. They are significantly lower than the previous upper limit of 2.3×10^{-5} [50], and in reasonable agreement with predictions [17], thus excluding the possibility of large ($O(10^2)$) enhancements from R-parity violating supersymmetric scenarios [51]. Their ratio can be determined directly from our data with greater accuracy than the individual values. For this purpose, the additional $p_T > 6 \text{ GeV}/c$ requirement is not necessary, and we can exploit the full sample size, obtaining $\mathcal{B}(\Lambda_b^0 \rightarrow p\pi^-)/\mathcal{B}(\Lambda_b^0 \rightarrow pK^-) = 0.66 \pm 0.14 \pm 0.08$, in good agreement with the predicted range 0.60–0.62 [17], but in disagreement with the recent prediction in Ref. [52].

The dominant systematic uncertainties of all measurements presented here are due to finite size of control samples and are expected to reduce with future extensions of the measurements.

In summary, we have searched for rare charmless decay modes of neutral b -hadrons into pairs of charged hadrons in CDF data. We report the first observation of the modes $B_s^0 \rightarrow K^-\pi^+$, $\Lambda_b^0 \rightarrow p\pi^-$, and $\Lambda_b^0 \rightarrow pK^-$, and measure their relative branching fractions. We set upper limits on the unobserved modes $B^0 \rightarrow K^+K^-$ and $B_s^0 \rightarrow \pi^+\pi^-$.

REFERENCES

- [1] R. FLEISCHER, *Phys.Lett.B*, **459** (1999) 306, arXiv:hep-ph/9903456.
- [2] A. SONI and D.A. SUPRUN, *Phys.Rev.D*, **75** (2006) 054006, arXiv:hep-ph/0609089.

- [3] M. GRONAU, *Phys.Lett.B*, **492** (2000) 297, arXiv:hep-ph/0008292.
- [4] H. J. LIPKIN, *Phys.Lett.B*, **621** (2005) 126, arXiv:hep-ph/0503022.
- [5] A. ABULENCIA *et al.*(CDF COLLABORATION), *Phys.Rev.Lett.*, **97** (2006) 211802, arXiv:hep-ex/0607021.
- [6] M. GRONAU and D. WYLER, *Phys.Lett.B*, **265** (1991) 172.
- [7] D. ATWOOD, I. DUNIETZ and A. SONI, *Phys.Rev.Lett.*, **78** (1997) 3257, arXiv:hep-ph/9612433; D. ATWOOD, I. DUNIETZ and A. SONI, *Phys.Rev.D*, **63** (2001) 036005, arXiv:hep-ph/0008090.
- [8] B. AUBERT *et al.*(BABAR COLLABORATION), *Phys.Rev.Lett.*, **93** (2004) 131801, arXiv:hep-ex/0407057; Y. CHAO *et al.*(BELLE COLLABORATION), *Phys.Rev.Lett.*, **93** (2004) 191802, arXiv:hep-ex/0408100.
- [9] Y.Y. KEUM and A.I. SANDA, *Phys.Rev.D*, **67** (2003) 054009, arXiv:hep-ph/0209014.
- [10] M. BENEKE, *Nucl.Phys.B*, **606** (2001) 245-321, arXiv:hep-ph/0104110.
- [11] M. GRONAU and J.L. ROSNER, *Phys.Rev.D*, **71** (2005) 074019, arXiv:hep-ph/0503131.
- [12] M. BENEKE and M. NEUBERT, *Nucl.Phys.B*, **675** (2003) 333, arXiv:hep-ph/0308039.
- [13] A. ALI, *Phys.Rev.D*, **76** (2007) 074018, arXiv:hep-ph/0703162;
- [14] X.-Q. YU, Y. LI and C.-D. LÜ, *Phys.Rev.D*, **71** (2005) 074026, erratum-ibidem *Phys.Rev.D*, **72** (2005) 119903, arXiv:hep-ph/0501152.
- [15] A. WILLIAMSON and J. ZUPAN, *Phys.Rev.D*, **74** (2006) 014003 erratum-ibidem *Phys.Rev.D*, **74** (2006) 03901, arXiv:hep-ph/0601214.
- [16] A. BURAS *et al.*, *Nucl.Phys.B*, **697** (2004) 133, arXiv:hep-ph/0402112.
- [17] R.MOHANTA *et al.*, *Phys.Rev.D*, **63** (2001) 074001, arXiv:hep-ph/0006109.
- [18] M.J. MORELLO, Ph. D. thesis, Scuola Normale Superiore, Pisa, FERMILAB-THESIS-2007-57 (2007).
- [19] T. AALTONEN *et al.*(CDF COLLABORATION), *Phys.Rev.Lett.*, **103** (2009) 031801, arXiv:0812.4271 [hep-ex].
- [20] D. ACOSTA *et al.* (CDF COLLABORATION), *Phys.Rev.D*, **71** (2005) 032001, arXiv:hep-ex/0412071.
- [21] CDF COLLABORATION, FERMILAB-PUB-96/390-E (1996).
- [22] A. SILL *et al*, *Nucl.Instrum.Meth.A*, **447** (2000) 1.
- [23] T. AFFOLDER *et al*, *Nucl.Instrum.Meth.A*, **42586** (2004) 249.
- [24] D. ACOSTA *et al*, *Nucl. Instrum. Meth. A*, **518** (2004) 605.
- [25] L. BALK *et al*, *Nucl.Instrum.Meth.A*, **267** (1988) 272.
- [26] S. BERTOLUCCI *et al*, *Nucl.Instrum.Meth.A*, **267** (1988) 301.
- [27] Y. SEIYA *et al*, *Nucl.Instrum.Meth.A*, **480** (2002) 524.
- [28] D. ACOSTA *et al*, *Nucl.Instrum.Meth.A*, **461** (2001) 540.
- [29] Isolation is defined as $I_B = p_T(B)/(p_T(B) + \sum_i p_{Ti})$, where $p_T(B)$ is the transverse momentum of the B candidate, and the sum runs over all other tracks within a cone of radius 1, in η - ϕ space around the B flight-direction.
- [30] G. PUNZI, eConf **C030908**, MODT002 (2003), arXiv:physics/0308063.
- [31] For a discussion of the bias in multi-component fits related to the use of multiple variables see G. PUNZI, eConf **C030908**, WELT002 (2003), arXiv:physics/0401045.
- [32] E. BARACCHINI and G. ISIDORI, *Phys.Lett.B*, **633** (2006) 309, arXiv:hep-ph/0508071.
- [33] D. ACOSTA *et al.* (CDF COLLABORATION), *Phys.Rev.Lett.*, **96** (2006) 202001, arXiv:hep-ex/0508022.
- [34] $A(x; c_2, m_0) = \text{Norm}[xe^{-c_2(\frac{x}{m_0})^2} \sqrt{1 - (\frac{x}{m_0})^2}]$ if $x \leq m_0$, $A(x; c_2, m_0) = 0$ if $x > m_0$.
- [35] We use frequentist limits based on Gaussian distribution of fit pulls (with systematics added in quadrature), and LR-ordering; see G. J. FELDMAN AND R. D. COUSINS, *Phys.Rev.D*, **57** (1998) 3873, arXiv:physics/9711021.
- [36] A. ABULENCIA *et al.* (CDF COLLABORATION), *Phys.Rev.Lett.*, **98** (2007) 122002, arXiv:hep-ex/0601003.
- [37] T. AALTONEN *et al.* (CDF COLLABORATION), *Phys.Rev.D*, **79** (2009) 032001, arXiv:0810.3213 [hep-ex].

- [38] D. ACOSTA *et al.* (CDF COLLABORATION), *Phys.Rev.Lett.*, **94** (2005) 122001, arXiv:hep-ex/0504006.
- [39] M. BENEKE *et al.*, *Phys.Lett.B*, **459** (1999) 631, arXiv:hep-ph/9808385.
- [40] A. LENZ, arXiv:hep-ph/0412007.
- [41] S. BIANCO, F. L. FABBRI, D. BENSON, and I. BIGI, *Riv.Nuovo Cim.*, **26N7** (2003) 1-200, arXiv:hep-ex/0309021.
- [42] B. AUBERT *et al.* (BABAR COLLABORATION), *Phys.Rev.Lett.*, **100** (2008) 061803, arXiv:0709.2715 [hep-ex]; M. STARIC *et al.* (BELLE COLLABORATION), *Phys.Lett.B*, **670** (2008) 190-195, arXiv:0807.0148 [hep-ex].
- [43] C. AMSLER *et al.*, *Phys.Lett.B*, **667** (2008) 1.
- [44] B. AUBERT *et al.* (BABAR COLLABORATION), *Phys.Rev.D*, **75** (2007) 012008, arXiv:hep-ex/0608003; K. ABE *et al.* (BELLE COLLABORATION), *Phys.Rev.Lett.*, **99** (2007) 121601, arXiv:hep-ex/0609015; A. BORNHEIM *et al.* (CLEO COLLABORATION), *Phys.Rev.D*, **68** (2003) 052002, arXiv:hep-ex/0302026.
- [45] J.-F. SUN, G.-H. ZHU and D.-S. DU, *Phys.Rev.D*, **68** (2003) 054003, arXiv:hep-ph/0211154.
- [46] C.-W. CHIANG, M. GRONAU, and J. L. ROSNER, *Phys.Lett.B*, **664** (2008) 169, arXiv:0803.3229 [hep-ph].
- [47] Y. LI, C.-D. LU, Z.-J. XIAO, and X.-Q. YU, *Phys.Rev.D*, **70** (2004) 034009, arXiv:hep-ph/0404028.
- [48] THE BELLE COLLABORATION, *Nature*, **452** (2008) 332.
- [49] B. AUBERT *et al.* (BABAR COLLABORATION), arXiv:0807.4226 [hep-ex].
- [50] D. E. ACOSTA *et al.*, (CDF COLLABORATION), *Phys.Rev.D*, **72** (2005) 051104, arXiv:hep-ex/0507067.
- [51] R. MOHANTA, *Phys.Rev.D*, **63** (2001) 056006, arXiv:hep-ph/0005240.
- [52] WEI, ZHENG-TAO and KE, HONG-WEI AND LI, XUE-QIAN, *Phys.Rev.D*, **80** (2009) 094016, arXiv:0909.0100 [hep-ph].